Sensor and Simulation Notes

Note 432

9 December 1998

Antenna Aperture with Tapered Loading for Waveform Control

Carl E. Baum
Air Force Research Laboratory
Directed Energy Directorate

Abstract

In designing pulse-radiating antennas for broadbeam applications (as in synthetic aperture radar) the frequency spectral properties of the pulse need to be controlled for the various angles. This paper considers a type of aperture antenna for this purpose. Noting the presence of spectral notches on boresight for a simple circular metal reflector, the reflector is resistively loaded in special ways to preserve the initial step rise of the far field (associated with step excitation) but smooth the pulse decay to remove the second step associated with the aperture rim.

1. Introduction

In designing antennas for synthetic aperture radar (SAR) one wants a sufficiently broad pattern to take appropriate advantage of the measurements of the scattering from a target while the antenna moves over a large distance (and thereby obtains a fine angular resolution via the large synthetic aperture). A SAR can also be designed to use a pulse containing a very large band of frequencies [13]. The pattern of an antenna can be different at each frequency depending on the specific type of antenna. One would like the pattern to be consistent at the various frequencies of interest in the pulse. An important consideration in the pattern is polarization and its control over the angles of interest in the pattern. Symmetry can help in this regard [7].

In designing a wide-angle pulse-radiating antenna one needs to be concerned with the radiated spectrum. Specifically, one would not like some important frequencies to be missing (notches). The frequencies of such notches may be a function of the angles from the antenna.

While an impulse-radiating antenna (IRA) can have good spectral properties on boresight [6, 12], it is designed to have a narrow beam width. One can achieve a broader beam width from a wide-angle TEM horn or from a TEM-fed hyperboloidal scatterer, which converts one spherical TEM wave into a second one [4]. On boresight, as we shall see, such an antenna radiates a pulse, which is not an impulse, but a gate function (step up followed by step down). Such a function has spectral notches at frequencies for which the pulse width is an integer number of sinusoidal periods.

As a special case, this paper considers the limiting case of a hyperboloid as a flat perfectly conducting circular disk. Noting the character of the boresight radiation, the disk is resistively loaded. Using a high-frequency approximation for the reflection from a resistive sheet, the appropriate aperture integral for the boresight-radiated field is performed. The radial variation of the sheet resistance is adjusted to control the waveform so that there is still the initial step rise, but this is followed by a smooth decay to zero, avoiding the second step.

Figure 1.1A shows the configuration of interest. A spherical TEM wave is launched from the source at $z = 2\ell$. A conical transmission line forming the spherical TEM wave is indicated; which precise form of the two or more conical conductors one may choose is left arbitrary for present purposes. A ray (high-frequency approximation) is indicated reflecting (negative sign) from the loaded aperture S_a on $z = \ell$. The reflected ray continues on a straight line passing through the coordinate origin ($\vec{r} = \vec{0}$). Figure 1.1B shows an equivalent problem (in the high-frequency approximation) in which the source is placed at $\vec{r} = \vec{0}$ with a reversal of the source voltage polarity on reflection of the feed through the aperture plane. Now there is a transmission of the field through the loaded aperture made to be the same in magnitude as in the first case. The resulting fields transmitted/reflected at S_a are discussed in Appendix C. Note that the low-frequency performance of the two antennas in Fig. 1.1 is quite different from radiation in the z direction due to the reversal of the electric dipole moment without reversing the magnetic dipole moment [5].

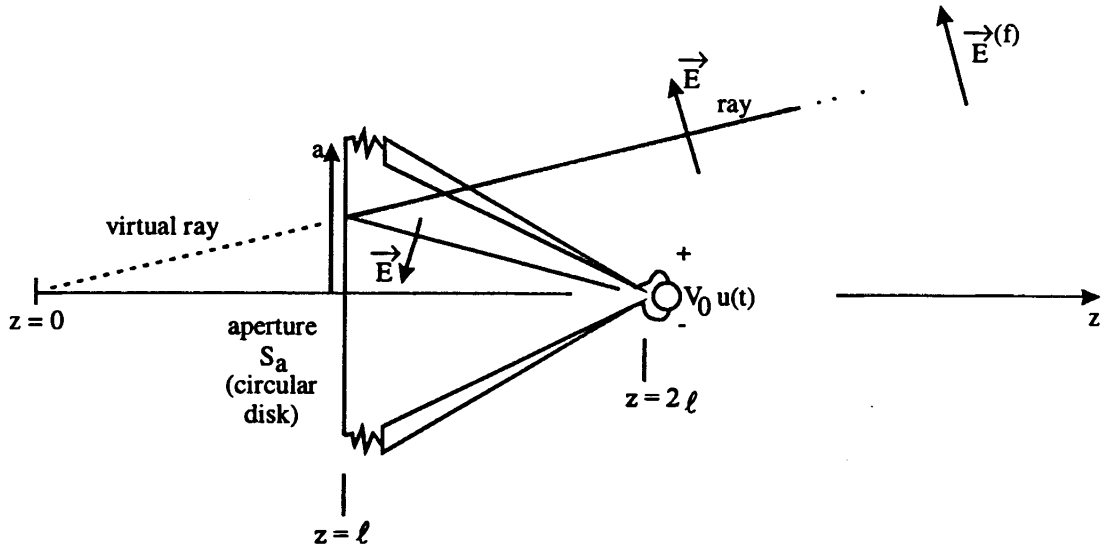

A. Circular disk reflector with controlled reflection

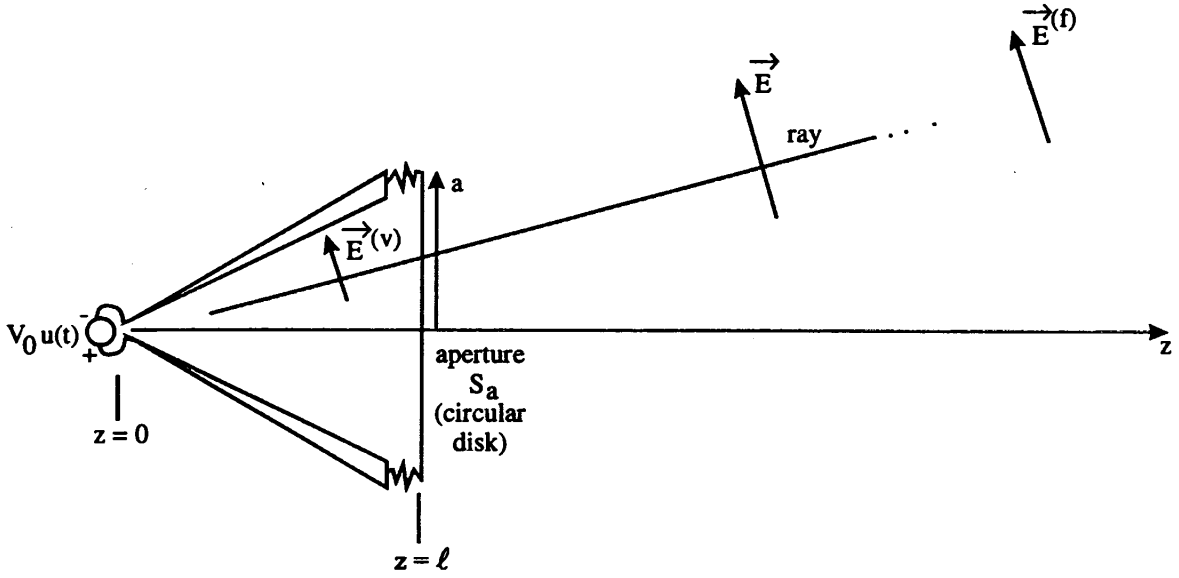

B. Horn with controlled transmittion

Fig. 1.1. TEM-Fed Loaded Planar Aperture.

For purposes of present analysis the configuration in Fig. 1.1B is more convenient due to the use of common coordinates for the fields on the feed, on S_a, and in the far field for $z \to \infty$. We have the usual cylindrical (Ψ, ϕ, z) and spherical coordinates (r, θ, ϕ) related to Cartesian coordinates (x, y, z) as

$$\begin{aligned} x &= \Psi\cos(\phi) \quad , \quad y = \Psi\sin(\phi) \\ \Psi &= r\sin(\theta) \quad , \quad z = r\cos(\theta) \end{aligned} \tag{1.1}$$

These are discussed in more detail in the appendices. The results will apply to the case in Fig. 1.1A as well, merely by the appropriate interpretation of transmission/reflection at S_a.

For our analysis we have the usual conventions

$$c = [\mu_0\varepsilon_0]^{-\frac{1}{2}} \equiv \text{speed of light}$$

$$Z_0 = \left[\frac{\mu_0}{\varepsilon_0}\right]^{-\frac{1}{2}} \equiv \text{wave impedance} \tag{1.2}$$

2. Spherical TEM Wave: Initial Considerations

Describing the problem in terms of the virtual feed in Fig. 1.1B, we have the fields to the left of S_a incident on S_a as an ideal step-function wave of the form

$$\vec{E}^{(v)}(\vec{r},t_r) = -\frac{V_0}{r\Delta\Phi}\nabla_s\Phi(\theta,\phi)u(t_r)$$

$$t_r = t - \frac{r}{c} \equiv \text{retarded time}$$

$$T_r \equiv ct_r \equiv \text{retarded time in length units} \qquad (2.1)$$

$$\Delta\Phi \equiv \text{change in potential function between feed conductors}$$

$$\nabla_s = \vec{1}_\theta\frac{\partial}{\partial\theta} + \vec{1}_\theta\csc(\theta)\frac{\partial}{\partial\phi}$$

The potential function satisfies the Laplace equation on the unit sphere and can be described as discussed in Appendix A.

The first simple way to view this problem is to imagine an observer on the z axis in the far field (large z). The first signal arrives as a step at $t_r = 0$. This corresponds to the field incident on S_a (with unity transmission) on the z axis, scaled by r^{-1}. It takes some extra time to reach the aperture edge at $\Psi = a$. This extra time in length units is

$$T_a \equiv ct_a = [\ell^2 + a^2]^{\frac{1}{2}} - \ell \qquad (2.2)$$

For an observer in the far field (on axis) this is the retarded time the observer first "sees" the truncation of the aperture at $\Psi = a$.

For simplicity, let us assume that the antenna has reflection symmetry R_y with respect to the $y = 0$ plane. The fields are taken as symmetric with respect to this plane [11]. On the z axis this means that the electric field is polarized in the y direction. Assuming that S_a is perfectly transparent (+1) in Fig. 1.1B, or perfectly reflecting (-1) in Fig. 1.1A, then we can write the far field on the z axis as [3]

$$\vec{E}^{(f)}(z\vec{1}_z,t_r) = \frac{\ell}{r}E_0\vec{1}_y[u(T_r) - u(T_r - T_a)]$$

$$\vec{E}_0 = E_0 \ \vec{1}_y = E^{(v)}(\ell \vec{1}_z, 0_+) \ \vec{1}_y \equiv \text{aperture field on } z \text{ axis for } t_r > 0 \tag{2.3}$$

The down step is an approximation since the aperture field is not only $\vec{E}^{(v)}$ after the aperture edge is reached (additional scattered fields). However, as we shall see, using this as the aperture field the aperture integral for the far field gives the above result.

3. Aperture Transmission/Reflection

Consistent with R_y symmetry, and for analytic simplification,, let the aperture loading be described by O_2 symmetry (all two-dimensional rotations and axial symmetry planes). Let the fields incident on S_a be weighted by the dyadic

$$\overleftrightarrow{W}(\Psi,\phi) = W_\Psi(\Psi)\,\vec{1}_\Psi\,\vec{1}_\Psi + W_\phi(\Psi\,\vec{1}_\phi\,\vec{1}_\phi) \tag{3.1}$$

This can be used to describe the transmission or reflection of the feed wave at S_a as desired.

Appendix C has the formulae to compute W_Ψ and W_ϕ for the applicable case based on sheet resistances R_{s1} and R_{s2}. Note that W_Ψ corresponds to the E wave and hence R_{s1}, while W_ϕ corresponds to the H wave and hence R_{s2}. The angle of incidence θ also corresponds to the θ of the spherical coordinates used here.

Various choices for $\overleftrightarrow{W}$ can be made consistent with (3.1) with

$$0 \le W_\Psi \le 1 \quad , \quad 0 \le W_\phi \le 1 \tag{3.2}$$

The two components can even be made the same. Note, however, that if one wishes to have the resistive sheet isotropic, then the two components above are in general different, except for small θ (as an approximation).

4. Far Field Computed from Aperture Integral

The far electric field specialized to the z axis is [2]

$$\vec{E}^{(f)}(z\vec{1}_z,t_r) = \frac{1}{2\pi cr}\frac{\partial}{\partial t}\int_{S_a}\vec{E}_t^{(a)}(\Psi,\phi;t-\frac{r_a}{c})d\,S_a$$

$$\begin{aligned}
\vec{E}_t^{(a)}(\Psi,\phi;t) &\equiv \text{tangential electric field on aperture} \\
&= \overleftrightarrow{W}(\Psi,\phi)\cdot\vec{E}^{(v)}(\Psi,\phi;t) \\
&= W_\Psi(\Psi)\cos(\theta)\,E_\theta^{(v)}(\Psi,\phi;t) + W_\phi(\Psi)\,E_\phi^{(v)}(\Psi,\phi;t) \\
r_a &= [\ell^2+\Psi^2]^{\frac{1}{2}} = r \text{ on aperture } S_a \\
t-\frac{r_a}{c} &\equiv \text{retarded time on aperture } S_a
\end{aligned} \tag{4.1}$$

Note that $r-\ell$ becomes r in the far-field asymptotics. Note also the inclusion of $\cos(\theta)$ accounting for $\vec{1}_\Psi\cdot\vec{1}_\theta$. Various details are discussed in Appendix B.

Converting retarded time to distance units we have

$$\begin{aligned}
\vec{E}^{(f)}(z\vec{1}_z,t_r) &= \frac{1}{2\pi r}\frac{\partial}{\partial T_r}\int_{S_a}\vec{E}_t^{(a)}(\Psi,\phi;t-\frac{r_a}{c})d\,S_a \\
&= \frac{1}{2\pi r}\frac{\partial}{\partial T_r}\int_0^a\int_0^{2\pi}\vec{E}_t^{(a)}(\Psi,\phi;t-\frac{r_a}{c})\Psi d\phi d\Psi
\end{aligned} \tag{4.2}$$

Substituting from (2.1) in terms of the potential function we have

$$\vec{E}^{(f)}(z\vec{1}_z,t_r) = -\frac{1}{2\pi r}\frac{V_0}{\Delta\Phi}\frac{\partial}{\partial T_r}\int_0^{\Psi_r}\int_0^{2\pi}\frac{1}{r_a}\overleftrightarrow{W}(\Psi,\phi)\cdot\nabla_s\Phi(\theta,\phi)\Psi d\phi d\Psi$$

$$\Psi_r = \begin{cases} 0 \text{ for } T_r<0 \\ \left[[\ell+T_r]^2 - -\ell^2\right]^{\frac{1}{2}} \text{ for } 0<T_r<T_a \\ a \text{ for } T_r > T_a \end{cases} \tag{4.3}$$

$$T_a = [\ell^2+a]^{\frac{1}{2}} - \ell$$

Here Ψ_r is the circular radius illuminated on the aperture as a function of retarded time as seen by the far-field observer on the z axis.

From Appendix B we have the conversion of the θ coordinate to Ψ on the aperture. There we also observe that the integrals over ϕ as in (B.5) leave only the $m = 1$ terms in the field expansion on S_a, the other terms giving zero. Collecting terms we have

$$\vec{E}^{(f)}(z\,\vec{1}_z, t_r) = \frac{b_1}{r\Delta\Phi}\,\vec{1}_y \frac{\partial}{\partial T_r}\int_0^{\Psi_r}\left[W_\Psi(\Psi)[\ell^2 + \Psi^2]^{-\frac{1}{2}}\frac{\ell\,\Psi}{[\ell^2 + \Psi^2]^{\frac{1}{2}} + \ell} + W_\phi(\Psi)\,\Psi^{-1}\left[[\ell^2 + \Psi^2]^{\frac{1}{2}} - \ell\right]\right] d\Psi \tag{4.4}$$

Consistent with previous results we have chosen a_1 to be zero to give an electric field at the aperture center as in (2.3) and (B.4) to be oriented in the y direction. We then can identify

$$\vec{E}_0 = E_0\,\vec{1}_y = \frac{b_1}{\ell\Delta\Phi}\,\vec{1}_y \equiv \text{aperture field for } \Psi = 0 \text{ and } t_r > 0 \tag{4.5}$$

We also have

$$\begin{aligned}\frac{\partial\Psi_r}{\partial T_r} &= [\ell + T_r]\left[[\ell\ T_r]^2 - \ell^2\right]^{-\frac{1}{2}}[u(T_r) - u(T_r - T_a)] \\ &= \Psi_r^{-1}\left[\ell^2 + \Psi_r^2\right]^{\frac{1}{2}}[u(T_r) - u(T_r - T_a)]\end{aligned} \tag{4.6}$$

Combining these with (4.4) gives

$$\vec{E}^{(f)}(z\vec{1}_z,t_r) = \vec{E}_0\frac{\ell}{r}\left[W_\Psi(\Psi_r)\ell\left[\left[\ell^2+\Psi_r^2\right]^{\frac{1}{2}}+\ell\right]^{-1}\right.$$

$$\left. + W_\phi(\Psi_r)\frac{\left[\ell^2+\Psi_r^2\right]^{\frac{1}{2}}}{\Psi_r^2}\left[\ell^2+\Psi^2\right]^{\frac{1}{2}}-\ell\right][u(T_r)-u(T_r-T_a)] \tag{4.7}$$

$$= \vec{E}_0\frac{\ell}{r}\frac{W_\Psi(\Psi_r)\ell + W_\phi(\Psi_r)[\ell^2+\Psi_r^2]^{\frac{1}{2}}}{[\ell^2+\Psi_r^2]^{\frac{1}{2}}+\ell}[u(T_r)-u(T_r-T_a)]$$

The last factor $u(T_r)-u(T_r-T_a)$ is the gate function previously discussed. The W weighting factors are at our disposal for tailoring the shape of the waveform.

A special case of interest has

$$W_\Psi(\Psi) = W_\phi(\Psi) \equiv W(\Psi) \tag{4.8}$$

With (4.8) this conveniently gives

$$\begin{aligned}\vec{E}^{(f)}(z\vec{1}_z,t_r) &= \vec{E}_0\frac{\ell}{r}W(\Psi_r)[u(T_r)-u(T_r-T_a)] \\ &= \vec{E}_0\frac{\ell}{r}W([[\ell+T_r]^2-\ell^2]^{\frac{1}{2}})[u(T_r)-u(T_r-T_a)]\end{aligned} \tag{4.9}$$

If we let the weight be uniformly one, then

$$\vec{E}^{(f)}(z\vec{1}_z,t_r) = \vec{E}_0\frac{\ell}{r}[u(T_r)-u(T_r-T_a)] \tag{4.10}$$

reproducing the result in (2.3). Another simple waveform of interest has

$$W(\Psi_r) = 1 - \frac{T_r}{T_a} \text{ for } 0 < T_r < T_a$$

$$= 1 - \frac{[\ell^2 + \Psi_r^2]^{\frac{1}{2}} - \ell}{[\ell^2 + a^2]^{\frac{1}{2}} - \ell} \text{ for } 0 < \Psi_r < a \tag{4.11}$$

For small a/ℓ (or equivalently small θ) this becomes

$$W(\Psi_r) = 1 - \left[\frac{\Psi_r}{a}\right]^2 \left[1 + O\left(\left[\frac{a}{\ell}\right]^2\right)\right] \text{ as } \frac{a}{\ell} \to 0 \tag{4.12}$$
$$\text{for } 0 < \Psi_r < a$$

This special loading gives a waveform which rises as a step with a straight-line decay to zero at $T_r = T_a$. This avoids the second step, giving a discontinuous derivative instead. The required dyadic sheet resistance can be constructed from the results of Appendix C. For a reflector as in Fig. 1.1A, the resistance is zero at $\Psi = 0$ and infinite at $\Psi = a$, for both $R_{s\Psi}$ and $R_{s\phi}$.

Returning to (4.7) one need not assume that the two weight functions are the same. A simple triangular waveform as in (4.11) can still be achieved by using the more general form in (4.7) and equating it to $1 - T_r / T_a$. Using

$$\cos(\theta) = \ell[\ell^2 + \Psi_r^2]^{-\frac{1}{2}} \tag{4.13}$$

in the formulae of Appendix C with

$$R_{s1} = R_{s\Psi}(\Psi_r) \quad , \quad R_{s2} = R_{s\phi}(\Psi_r) \tag{4.14}$$

various $W_\Psi(\Psi_r)$ and $W_\phi(\Psi_r)$ can be synthesized from

$$\frac{W_\Psi(\Psi_r)\ell + W_\phi(\Psi_r)[\ell^2 + \Psi_r^2]^{\frac{1}{2}}}{[\ell^2 + \Psi_r^2]^{\frac{1}{2}} + \ell} = 1 - \frac{T_r}{T_a} \tag{4.15}$$

A special case has

$$R_{s\Psi}(\Psi_r) = R_{s\phi}(\Psi_r) = R_s(\Psi_r) \tag{4.16}$$

making the resistive sheet isotropic (but nonuniform). Except for small a/ℓ (small θ) then W_Ψ and W_ϕ are different, but (4.15) can be solved to find $R_s(\Psi_r)$, depending on whether the reflection (Fig. 1.1A) or transmission form (Fig. 1.1B) is desired.

5. Concluding Remarks

Here we have considered a canonical problem concerning aperture loading for broadbeam antennas for SAR using a pulse involving a broad band of frequencies. The resistively loaded aperture is planar in this canonical case. The function of the resistive loading is to improve the frequency spectrum of the pulse on boresight. Off boresight the edge of the aperture does not have the same effect as a second step, this signal being dispersed (not arriving simultaneously) at the observer.

For good low-frequency performance there is the question of optimal termination of the TEM feed. This has previously been considered in the context of various types of IRAs. With a resistively loaded aperture, the aperture resistance will need to be included as part of the termination.

There are other approaches to this spectral-control problem. One can shape the reflector (or contour the lens) so that in the central region the ideal flat-plate (or more generally hyperboloidal) region is retained, while deformed near the outer edge ($\Psi = a$). This will also disperse the second step to some degree (to be determined) as seen on boresight.

Appendix A. TEM Potentials and Fields

An important part of the antenna design concerns the properties of TEM waves, both planar and spherical, for their dispersionless characteristics. This includes potentials, fields, and associated operators.

A.1. Plane waves

In cylindrical coordinates on a plane with

$$x = \Psi\cos(\phi) \quad , \quad y = \Psi\sin(\phi) \tag{A.1}$$

We have a potential function of the form [10]

$$\Phi^{(p)}(\Psi,\phi) = \sum_{m=0}^{\infty}\left[\frac{\Psi}{\Psi_0}\right]^m \left[a_m\cos(m\phi) + b_m\sin(m\phi)\right]$$

$$\Psi_0 \equiv \text{arbitrary scaling constant (meters)} \tag{A.2}$$

This satisfies the Laplace equation on the plane as [9]

$$\nabla_p^2\Phi^{(p)}(\Psi,s) = \Psi^{-1}\frac{\partial}{\partial\Psi}\left[\Psi\frac{\partial\Phi^{(p)}(\Psi,s)}{\partial\Psi}\right] + \Psi^{-2}\frac{\partial^2\Phi^{(p)}(\Psi,\phi)}{\partial\phi^2} = 0 \tag{A.3}$$

Here we have not included negative powers of Ψ (or a logarithmic term) since we are considering the case that $\Phi^{(p)}$ is well behaved near $\Psi = 0$.

With the gradient we have

$$\begin{aligned}\nabla_p\,\Phi^{(p)}(\Psi,s) &= \frac{\partial\Phi^{(p)}(\Psi,\phi)}{\partial\Psi}\,\vec{1}_\Psi + \frac{1}{\Psi}\frac{\partial\Phi^{(p)}(\Psi,\phi)}{\partial\phi}\,\vec{1}_\phi \\ &= \Psi_0^{-1}\sum_{m=1}^{\infty} m\left[\frac{\Psi}{\Psi_0}\right]^{m-1}\Big[\left[a_m\cos(m\phi) + b_m\sin(m\phi)\right]\vec{1}_\phi \\ &\qquad + \left[-a_m\sin(m\phi) + b_m\cos(m\phi)\right]\vec{1}_\phi\Big]\end{aligned} \tag{A.4}$$

This can be used to expand electric and/or magnetic fields in a planar TEM wave.

A.2. Spherical waves

The functional expansion for plane waves in (A.2) can be converted to one for spherical waves by a stereographic projection [10] as

$$\Psi = 2\ell \tan\left(\frac{\theta}{2}\right) \tag{A.5}$$

where ℓ is the distance from the source ($r = 0$) to the projection plane, tangent at $\theta = 0$. Here spherical coordinates (r, θ, ϕ) are related to cylindrical coordinates (Ψ, ϕ, z) as

$$\Psi = r \sin(\theta) \quad , \quad z = r \cos(\theta) \tag{A.6}$$

with ϕ the same in both systems. For convenience we can set both ℓ and Ψ_0 to zero for potentials and fields on the unit sphere.

The potential function now takes the form

$$\Phi^{(s)}(\theta,\phi) = \sum_{m=0}^{\infty} \left[2 \tan\left(\frac{\theta}{2}\right)\right]^m [a_m \cos(m\phi) + b_m \sin(m\phi)] \tag{A.7}$$

and is well behaved near $\theta = 0$. For small θ this has the form

$$\Phi^{(s)}(\theta,\phi) = \sum_{m=0}^{\infty} \theta^m [a_m \cos(m\phi) + b_m \sin(m\phi)] + O(\theta^3) \text{ as } \theta \to 0 \tag{A.8}$$

recovering the form in (A.1) near the point the stereographic projection plane is tangent to the sphere. This spherical potential satisfies the Laplace equation on the unit sphere as [9]

$$\nabla_s^2 \Phi^{(s)}(\theta,\phi) = \csc(\theta) \frac{\partial}{\partial \theta}\left[\sin(\theta) \frac{\partial \Phi^{(s)}(\theta,\phi)}{\partial \theta}\right] \csc^2(\theta) \frac{\partial^2 \Phi^{(s)}(\theta,\phi)}{\partial \theta^2} = 0 \tag{A.9}$$

With the gradient we have

$$\nabla_s \Phi^{(s)}(\theta,\phi) = \frac{\partial \Phi^{(s)}(\theta,\phi)}{\partial \theta} \vec{1}_\theta + \csc(\theta) \frac{\partial \Phi^{(c)}(\theta,\phi)}{\partial \theta} \vec{1}_\phi$$

$$= \sum_{m=1}^{\infty} m \left[\left[2 \tan\left(\frac{\theta}{2}\right) \right]^{m-1} \sec^2\left(\frac{\theta}{2}\right) [a_m \cos(m\phi) + b_m \cos(m\phi)] \vec{1}_\theta \right. \tag{A.10}$$

$$\left. + \csc(\theta) \left[2 \tan\left(\frac{\theta}{2}\right) \right]^m [-a_m \sin(m\phi) + b_m \cos(m\phi)] \vec{1}_\theta \right]$$

This can be used to expand electric and/or magnetic fields in a spherical TEM wave.

Appendix B. Spherical TEM Potentials and Fields on Plane

Having the general form of a spherical TEM wave in terms of θ , ϕ on a unit sphere (Appendix A), we need to find the potential and tangential components of the fields on a plane. This plane is the antenna aperture plane (discussed previously) consisting of a plane at $z = \ell$. On this plane we have

$$\sin(\theta) = \Psi\left[\ell^2 + \Psi^2\right]^{-\frac{1}{2}} \quad , \quad \cos(\theta) = \ell\left[\ell^2 + \Psi^2\right]^{-\frac{1}{2}}$$

$$\tan(\theta) = \frac{\Psi}{\ell}$$

$$\tan\left(\frac{\theta}{2}\right) = \frac{1-\cos(\theta)}{\sin(\theta)} = \frac{\left[\ell^2 + \Psi^2\right]^{\frac{1}{2}} - \ell}{\Psi}$$

$$\cos^2\left(\frac{\theta}{2}\right) = \frac{1+\cos(\theta)}{2} = \frac{\left[\ell^2 + \Psi^2\right]^{\frac{1}{2}} + \ell}{2\left[\ell^2 + \Psi^2\right]^{\frac{1}{2}}}$$

$$\vec{1}_\theta = \cos(\theta)\,\vec{1}_\Psi - \sin(\theta)\,\vec{1}_z$$

$$\overleftrightarrow{1}_z \cdot \vec{1}_\theta = \cos(\theta)\,\vec{1}_\Psi$$

$$\vec{1}_\Psi = \cos(\phi)\,\vec{1}_x + \sin(\phi)\,\vec{1}_y \quad , \quad \vec{1}_\phi = -\sin(\phi)\,\vec{1}_x + \cos(\phi)\,\vec{1}_y$$

$$r_a = \left[\ell^2 + \Psi^2\right]^{\frac{1}{2}} \qquad \text{(B.1)}$$

$\equiv$ value of r on aperture plane (S_a) (to distinguish from r in far field)

As these are to be used in integrals over S_a we need to distinguish these coordinates from those for the fields away from S_a (evaluated by such integrals).

The potential evaluated on S_a then takes the form by substitution in (A.7) to give

$$\Phi^{(a)}(\Psi,\phi) = \sum_{m=0}^{\infty} \left[2\frac{\left[\ell^2 + \Psi^2\right]^{\frac{1}{2}} - \ell}{\Psi} \right]^m [a_m \cos(m\phi) + b_m \sin(m\phi)] \qquad \text{(B.2)}$$

For the fields tangential to we obtain from (A.10)

$$\frac{1}{r_a}\overleftrightarrow{1}_z \cdot \nabla_s \Phi^{(a)}(\Psi,\phi)$$

$$\sum_{m=1}^{\infty} m \left[\left[\ell^2+\Psi^2\right]^{-\frac{1}{2}} \left[2\frac{\left[\ell^2+\Psi^2\right]^{\frac{1}{2}}-\ell}{\Psi} \right]^{m-1} \frac{2\ell}{\left[\ell^2+\Psi^2\right]^{\frac{1}{2}}+\ell} [a_m \cos(m\phi)+b_m \sin(m\phi)] \vec{1}_\Psi \right. \tag{B.3}$$

$$\left. + \frac{1}{\Psi} \left[2\frac{\left[\ell^2+\Psi^2\right]^{\frac{1}{2}}-\ell}{\Psi} \right]^{m} [-a_m \sin(m\phi)+b_m \cos(m\phi)\ \vec{1}_\phi \right]$$

Note the factor of r_a^{-1}; this accounts for the decrease with r of the spherical TEM wave on S_a. The gradient is on the unit sphere, but the coordinates have been changed to Ψ,ϕ on S_a with the θ component projected as a Ψ component.

A special case of interest is on the z axis. For $\Psi = 0$ (and thereby $\theta = 0$) only the $m=1$ term is nonzero giving

$$\begin{aligned} &\frac{1}{r_a}\overleftrightarrow{1}_z \cdot \nabla_s \Phi^{(a)}(\Psi,\phi)\Big|_{\Psi=0} \\ &= \frac{1}{\ell}\left[[a_1 \cos(\phi) + b_1 \sin(\phi)] \vec{1}_\Psi + [-a_1 \sin(\phi)+b_1 \cos(\phi)] \vec{1}_\phi \right] \\ &= \frac{1}{\ell}[a_1 \vec{1}_x + b_1 \vec{1}_y] \end{aligned} \tag{B.4}$$

For the present problem the symmetry has the electric field in the y direction. This allows us to identify $b_1 \vec{1}_y/\ell$ with the electric field in the center of the aperture.

We need integrals over ϕ as

$$\int_0^{2\pi} [a_m \cos(m\phi)+b_m \sin(m\phi)] \vec{1}_\Psi \, d\phi$$

$$= \int_0^{2\pi} [a_m \cos(m\phi)+b_m \sin(m\phi)] \, [\cos(\phi) \vec{1}_x + \sin(\phi) \vec{1}_y] d\phi \, \vec{1}_\Psi \, d\phi$$

$$
\begin{aligned}
&= \begin{cases} \pi[a_1 \vec{1}_x + b_1 \vec{1}_y] & \text{for } m = 1 \\ \vec{0} & \text{for } m > 1 \end{cases} \\
&\int_0^{2\pi} [-a_m \sin(m\phi) + b_m \cos(m\phi)] \vec{1}_\phi \, d\phi \\
&= \int_0^{2\pi} [-a_m \sin(m\phi) + b_m \cos(m\phi)][-\sin(\phi) \vec{1}_x + \cos(\phi) \vec{1}_y] \, d\phi \\
&= \begin{cases} \pi[a_1 \vec{1}_x + b_1 \vec{1}_y] & \text{for } m = 1 \\ \vec{0} & \text{for } m > 1 \end{cases}
\end{aligned}
\tag{B.5}
$$

Only the $m = 1$ terms survive due to orthogonality. As in (B.4), if $a_1 = 0$ the above is polarized in the y direction.

Appendix C. Transmission and Reflection of Plane Wave at Resistive Sheet

For the fields at the antenna aperture we need the tangential electric field in the presence of a resistive sheet on plane S. As illustrated in Fig. C.1, the sheet is on a plane of constant z (consistent with earlier coordinates). The transverse dyadic is

$$\overleftrightarrow{1}_z = \overleftrightarrow{1} - \vec{1}_z \vec{1}_z \tag{C.1}$$

This is independent of which of two choices we take for positive z.

For the incident wave we take the orthogonal unit vectors

$$\begin{aligned} &\vec{1}_1 \times \vec{1}_2 = \vec{1}_3 \equiv \text{direction of incidence} \\ &\vec{1}_1 \equiv \text{vertical polarization (in plane of incidence)} \\ &\vec{1}_2 \equiv \text{horizontal polarization (parallel to } S_a) \end{aligned} \tag{C.2}$$

On S we also need

$$\begin{aligned} &\vec{1}_1' = \cos(\theta)\, \vec{1}_1 + \sin(\theta)\, \vec{1}_3 = \vec{1}_2 \times \vec{1}_z \\ &\theta \equiv \text{angle of incidence} \end{aligned} \tag{C.3}$$

The tangential fields on S are referenced to $\vec{1}_1'$ and $\vec{1}_2$, and θ is consistent with usage in earlier sections.

On S we have a resistive sheet which we take as uniform, but also as a dyadic of the form

$$\overleftrightarrow{R}_s = R_{s1}\, \vec{1}_1' \vec{1}_1' + R_{s2}\, \vec{1}_2 \vec{1}_2 \tag{C.4}$$

This makes R_{s1} apply to an E wave and R_{s2} to an H wave as indicated in Fig. A.1. Note also now that the transverse dyadic has the representation

$$\overleftrightarrow{1}_z = \vec{1}_1' \vec{1}_1' + \vec{1}_2 \vec{1}_2 \tag{C.5}$$

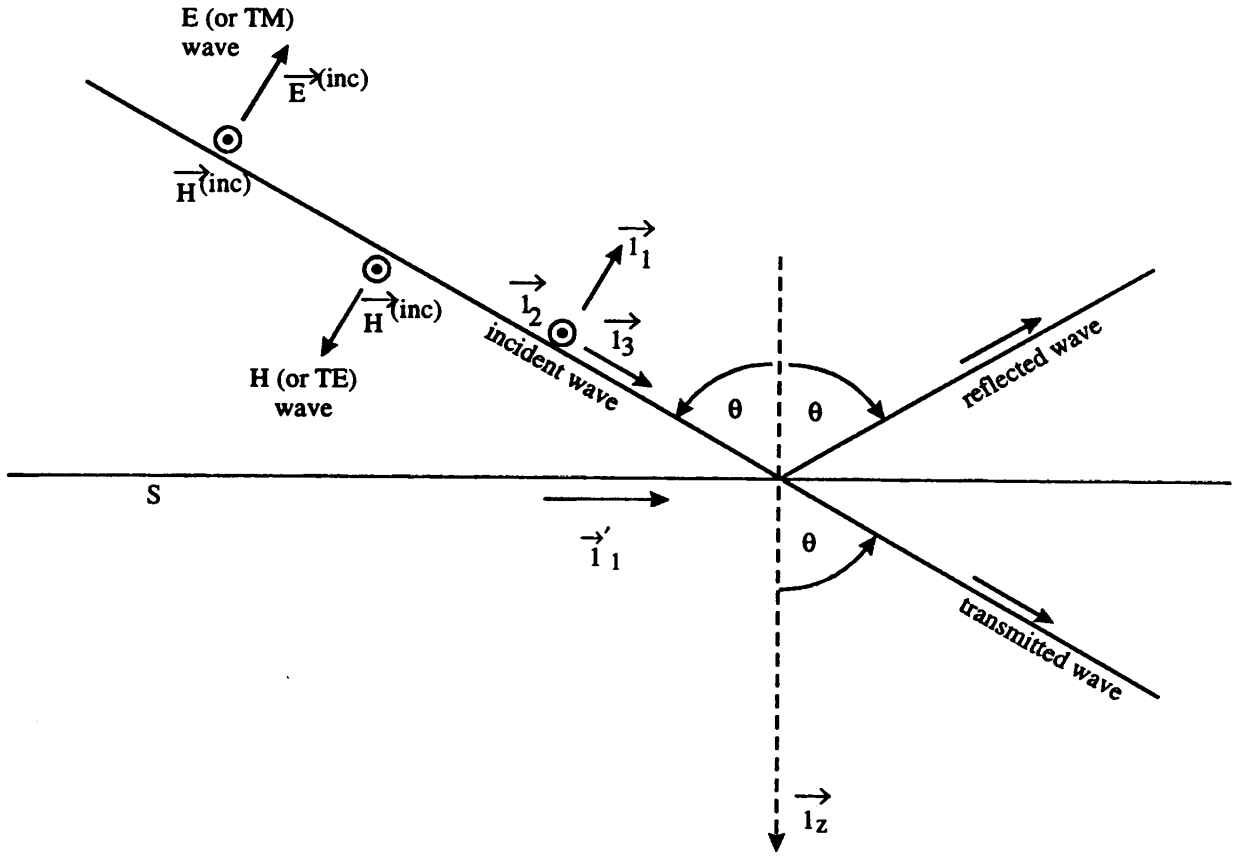

Fig. C.1. Plane Wave Incident on Resistive Sheet.

C.1. E wave

For an E wave we have the incident fields

$$\begin{aligned} \vec{E}^{(inc)} &= E^{(inc)}\,\vec{1}_1 \quad , \quad \vec{H}^{(inc)} = H^{(inc)}\,\vec{1}_2 \\ E^{(inc)} &= Z_0\, H^{(inc)} \end{aligned} \tag{C.6}$$

The tangential incident fields on S are

$$\begin{aligned} \vec{E}_t^{(inc)} &= \overleftrightarrow{1}_z \cdot \vec{E}^{(inc)} = \cos(\theta)\, E^{(inc)}\,\vec{1}'_1 \\ \vec{H}_t^{(inc)} &= \overleftrightarrow{1}_z \cdot \vec{H}^{(inc)} = H^{(inc)}\,\vec{1}_2 \end{aligned} \tag{C.7}$$

Our interest is in the resulting tangential electric field on S. For this we need the transmission coefficient for the transmitted wave; this applies both to the electric field referenced to $\vec{1}_1$, as well as the tangential part referenced to $\vec{1}'_1$. From [1, 8] we have

$$T_1 \equiv \frac{E^{(trans)}}{E^{(inc)}} = \frac{E_t^{(trans)}}{E_t^{(inc)}} = \left[1 + \frac{Z_0}{2R_{s1}}\cos(\theta)\right]^{-1} \tag{C.8}$$

This applies to the transmission case in Fig. 1.1B. For interpreting the case of reflected fields as in Fig. 1.1A we have the corresponding reflection coefficient.

$$R_1 = \frac{E^{(refl)}}{E^{(inc)}} = \frac{E_t^{(refl)}}{E_t^{(inc)}} = -\left[1 + \frac{2R_{s1}}{Z_0}\sec(\theta)\right]^{-1} = T_1 - 1 \tag{C.9}$$

C.2. H wave

For an H wave we have the incident field

$$\begin{aligned} \vec{E}^{(inc)} &= E^{(inc)}\,\vec{1}_2 \quad , \quad \vec{H}^{(inc)} = -H^{(inc)}\,\vec{1}_1 \\ E^{(inc)} &= Z_0\, H^{(inc)} \end{aligned} \tag{C.10}$$

The tangential incident fields on S are

$$\begin{aligned} \vec{E}_t^{(inc)} &= \overleftrightarrow{1}_z \cdot \vec{E}^{(inc)} = E^{(inc)} \vec{1}_2 \\ \vec{H}_t^{(inc)} &= \overleftrightarrow{1}_z \cdot \vec{H}^{(inc)} = -\cos(\theta) H^{(inc)} \vec{1}'_1 \end{aligned} \tag{C.11}$$

In this case the transmission coefficient for the electric field (which is also the tangential part) referenced to $\vec{1}_2$ is [1, 8]

$$T_2 \equiv \frac{E^{(trans)}}{E^{(inc)}} = \left[1 + \frac{Z_0}{2R_{s2}} \sec(\theta)\right]^{-1} \tag{C.12}$$

For use with reflected fields at S_a we have the corresponding reflection coefficient

$$R_2 = \frac{E^{(refl)}}{E^{(inc)}} = -\left[1 + \frac{2R_2}{Z_0} \cos(\theta)\right]^{-1} = T_2 - 1 \tag{C.13}$$

C.3. Transmission and reflection dyadics

For a combination of E and H waves incident on S at common angle θ we have the transmission dyadic

$$\begin{aligned} \overleftrightarrow{T} &= T_1 \vec{1}'_1 \vec{1}'_1 + T_2 \vec{1}_2 \vec{1}_2 \\ &= \left[1 + \frac{Z_0}{2R_{s1}} \cos(\theta)\right]^{-1} \vec{1}'_1 \vec{1}'_1 + \left[1 + \frac{Z_0}{2R_{s2}} \sec(\theta)\right]^{-1} \vec{1}_2 \vec{1}_2 \end{aligned} \tag{C.14}$$

Note that T_1 and T_2 are, in general, different and can be independently specified if one is willing to construct an anisotropic resistive sheet (say, by a fine grid of resistors). If one wishes to equate T_1 and T_2 we have a constraint

$$\frac{R_{s2}}{R_{s1}} = \sec^2(\theta) \tag{C.15}$$

Note that for small θ this gives

$$\frac{R_{s2}}{R_{s1}} = 1 + O(\theta) \text{ as } \theta \to 0 \tag{C.16}$$

So for small θ , one can approximate this constraint by a uniform isotropic resistive sheet.

One can similarly construct a reflection dyadic as

$$\begin{aligned}\overleftrightarrow{R} &= R_1 \vec{1}'_1 \vec{1}'_1 + R_2 \vec{1}_2 \vec{1}_2 \\ &= -\left[1+\frac{2R_{s1}}{Z_0}\sec(\theta)\right]^{-1} \vec{1}'_1 \vec{1}'_1 - \left[1+\frac{2R_{s2}}{Z_0}\cos(\theta)\right]^{-1} \vec{1}'_2 \vec{1}'_2\end{aligned} \tag{C.17}$$

Equations (C.15) and (C.16) apply equally well to this case.

References

1. D. V. Giri, C. E. Baum, and H. Schilling, Electromagnetic Considerations of a Spatial Modal Filter for Suppression of Non-TEM Modes in the Transmission-Line Type of EMP Simulators, Sensor and Simulation Note 247, December 1978.

2. C. E. Baum, Aperture Efficiencies for IRAs, Sensor and Simulation Note 328, June 1991.

3. E. G. Farr and C. E. Baum, A Simple Model of Small-Angle TEM Horns, Sensor and Simulation Note 340, May 1992.

4. C. E. Baum and E. G. Farr, Hyperboloidal Scatterer for Spherical TEM Waves, Sensor and Simulation Note 343, July 1992.

5. C. E. Baum, Low-Frequency-Compensated TEM Horn, Sensor and Simulation Note 377, January 1995.

6. D. V. Giri, Radiated Spectra of Impulse Radiating Antennas (IRAs), Sensor and Simulation Note 386, November 1995.

7. C. E. Baum, Symmetry in SAR Antennas, Sensor and Simulation Note 431, November 1998.

8. C. E. Baum, Damping Transmission-Line and Cavity Resonances, Interaction Note 503, May 1994.

9. J. Van Bladel, *Electromagnetic Fields*, Hemisphere Publishing Corp. (Taylor & Francis), 1985.

10. W. R. Smythe, *Static and Dynamic Electricity*, Hemisphere Publishing Corp. (Taylor & Francis), 1989.

11. C. E. Baum and H. N. Kritikos, Symmetry in Electromagnetics, Ch. 1, pp. 1-90, in C. E. Baum and H. N. Kritikos, *Electromagnetic Symmetry*, Taylor & Francis, 1995.

12. D. V. Giri and C. E. Baum, Temporal and Spectral Radiation on Boresight of a Reflector Type of Impulse Radiating Antenna (IRA), pp. 65-72, in C. E. Baum et al (eds.), *Ultra-Wideband, Short-Pulse Electromagnetics 3*, Plenum, 1997.

13. J. McCorkle, V. Sabio, R. Kapoor, and N. Nandhakumar, Transient Synthetic Aperture Radar and the Extraction of Anisotropic and Natural Frequency Information, Ch. 12, pp. 375-430, in C. E. Baum (ed.), *Detection and Identification of Visually Obscured Targets*, Taylor & Francis, 1998.